JOURNAL OF GEOPHYSICAL RESEARCH, VOL. 112, B06412, doi:10.1029/2006JB004628, 2007

Click Here for Full Article

Bathymetry of the Pacific plate and its implications for thermal evolution of lithosphere and mantle dynamics

Shijie Zhong,[1] Michael Ritzwoller,[1] Nikolai Shapiro,[2] William Landuyt,[3] Jinshui Huang,[4] and Paul Wessel[5]

Received 13 July 2006; revised 10 January 2007; accepted 2 March 2007; published 21 June 2007.

[1] A long-standing question in geodynamics is the cause of deviations of ocean depth or seafloor topography from the prediction of a cooling half-space model (HSC). Are the deviations caused entirely by mantle plumes or lithospheric reheating associated with sublithospheric small-scale convection or some other mechanisms? In this study we analyzed the age and geographical dependences of ocean depth for the Pacific plate, and we removed the effects of sediments, seamounts, and large igneous provinces (LIPs), using recently available data sets of high-resolution bathymetry, sediments, seamounts, and LIPs. We found that the removal of seamounts and LIPs results in nearly uniform standard deviations in ocean depth of ~300 m for all ages. The ocean depth for the Pacific plate with seamounts, LIPs, the Hawaiian swell, and South Pacific super-swell excluded can be fit well with a HSC model till ~80–85 Ma and a plate model for older seafloor, particularly, with the HSC-Plate depth-age relation recently developed by Hillier and Watts (2005) with an entirely different approach for the North Pacific Ocean. A similar ocean depth-age relation is also observed for the northern region of our study area with no major known mantle plumes. Residual topography with respect to Hillier and Watts' HSC-Plate model shows two distinct topographic highs: the Hawaiian swell and South Pacific super-swell. However, in this residual topography map, the Darwin Rise does not display anomalously high topography except the area with seamounts and LIPs. We also found that the topography estimated from the seismic model of the Pacific lithosphere of Ritzwoller et al. (2004) generally agrees with the observed topography, including the reduced topography at relatively old seafloor. Our analyses show that while mantle plumes may be important in producing the Hawaiian swell and South Pacific super-swell, they cannot be the only cause for the topographic deviations. Other mechanisms, particularly lithospheric reheating associated with "trapped" heat below old lithosphere (Huang and Zhong, 2005), play an essential role in causing the deviations in topography from the HSC model prediction.

Citation: Zhong, S., M. Ritzwoller, N. Shapiro, W. Landuyt, J. Huang, and P. Wessel (2007), Bathymetry of the Pacific plate and its implications for thermal evolution of lithosphere and mantle dynamics, *J. Geophys. Res.*, *112*, B06412, doi:10.1029/2006JB004628.

1. Introduction

[2] Seafloor topography (i.e., ocean depth) and heat flux are the key observations that reflect the thermal and dynamic states of the mantle and lithosphere. Seafloor topography increases with the age of seafloor (i.e., lithospheric age), while seafloor heat flux decreases with lithospheric age. Seafloor topography and heat flux can be explained to first order as a result of conductive cooling and thermal contraction of initially hot oceanic lithosphere [e.g., *McKenzie*, 1967; *Parsons and Sclater*, 1977; *Lister et al.*, 1990]. In particular, it has been suggested that a half-space cooling (HSC) model reproduces seafloor topography for seafloor younger than 70 Ma [*Parsons and Sclater*, 1977] and heat flux data for seafloor younger than 110 Ma [*Lister et al.*, 1990]. However, for older seafloor the observations show reduced dependence on the age in comparison with the HSC model predictions [*Parsons and Sclater*, 1977; *Lister et al.*, 1990].

[3] Understanding the origin of the deviations of seafloor topography and heat flux from the HSC model is a key to understanding the dynamics of the mantle. Two main proposals have been suggested to explain the deviations: large-scale mantle convective upwellings associated with deep mantle processes and lithospheric reheating (i.e., a plate model) related to shallow mantle processes. First, the

[1]Department of Physics, University of Colorado, Boulder, Colorado, USA.
[2]Institut de Physique du Globe, Paris, France.
[3]Department of Geology and Geophysics, Yale University, New Haven, Connecticut, USA.
[4]Research School of Earth Sciences, Australian National University, Canberra, ACT, Australia.
[5]Department of Geology and Geophysics, School of Ocean and Earth Science and Technology, University of Hawaii at Manoa, Honolulu, Hawaii, USA.

Copyright 2007 by the American Geophysical Union.
0148-0227/07/2006JB004628$09.00

deviations are often explained in terms of a plate model. In the plate model it is suggested that the lithosphere ceases cooling when it reaches a certain age and thickness [*Parsons and Sclater*, 1977], distinct from the HSC model in which the cooling of the lithosphere may continue indefinitely until subduction at oceanic trenches. The plate model assumes either a constant temperature [*Parsons and Sclater*, 1977; *Stein and Stein*, 1992] or a constant heat flux [*Doin and Fleitout*, 2000; *Dumoulin et al.*, 2001] at the base of the lithosphere, but does not directly address the physical processes that may be responsible for the required conditions at the base of the lithosphere (i.e., the plate model is basically a curve fitting). A commonly suggested mechanism for the plate model is thermal boundary layer instabilities (i.e., sublithospheric small-scale convection or SSC) that may occur dynamically below relatively old lithosphere [*Parsons and McKenzie*, 1978; *Yuen and Fleitout*, 1985; *Davaille and Jaupart*, 1994]. The SSC acts to destabilize the bottom part of the lithosphere and replace it with the relatively hot mantle (i.e., lithospheric reheating), thus preventing the lithosphere from continuous cooling.

[4] Second, large-scale convective processes associated with the deep mantle, in particular upwelling mantle plumes, may also cause topographic anomalies that may lead to deviations from the HSC model [*Davies*, 1988a; *Davies and Pribac*, 1993; *Sleep*, 1990; *Lithgow-Bertelloni and Silver*, 1998; *McNutt*, 1998]. Mantle plumes result from thermal boundary layer instabilities in the deep mantle, possibly at the core-mantle boundary (CMB) [*Morgan*, 1972], and the plume mode of convection is essential for cooling the core [e.g., *Davies*, 1988a; *Sleep*, 1990]. A number of seismic studies have also found evidence for mantle plumes [*Wolfe et al.*, 1997; *Romanowicz and Gung*, 2002; *Montelli et al.*, 2004]. Mantle plumes, owing to their buoyancy forces, may produce topographic highs, and the best example is probably the Hawaiian swell topography that is suggested to result from the Pacific plate moving over a plume [*Davies*, 1988a; *Sleep*, 1990].

[5] Questions, however, have been raised about the applicability of the plate/SSC model and even the generality of the topographic deviations from the HSC model:

[6] 1. *Heestand and Crough* [1981] and *Schroeder* [1984] indicated that seafloor topography could be fit to the HSC model if the areas affected by seamounts and mantle plumes are excluded in topography analyses. *Marty and Cazenave* [1989] further demonstrated that the depth-age relation depends on the oceans and regions and that in some regions the topography follows the HSC model predictions to much older seafloor ages. These studies suggest that the topographic deviations from the HSC model are just regional features, thus questioning the necessity of the plate model.

[7] 2. *O'Connell and Hager* [1980] and *Davies* [1988b, 1999] suggested that the SSC, the physical mechanism for the plate model, may not lead to reduced topography, because the SSC enhances the cooling of the underlying mantle and this may offset any effects of lithospheric reheating from the SSC on the topography.

[8] 3. Some of the topographic deviations from the HSC model predictions, including the Hawaiian swell are location-dependent and are not directly related to lithospheric age. Therefore the plate/SSC model, with lithospheric age as the sole variable, cannot account for all the topographic deviations [e.g., *Panasyuk and Hager*, 2000].

[9] The purpose of this study is to examine the controls on seafloor topography and to understand the causes of the topographic deviations. We analyze the age and geographical dependences of ocean depth for the Pacific plate, and we remove the effects of sediments, seamounts, and LIPs, using recently available data sets of high-resolution bathymetry, sediments, seamounts, and LIPs. We compare the corrected topography with predictions from the HSC and plate models and examine its correlation with recent seismic models for the Pacific lithosphere and shallow upper mantle [*Ritzwoller et al.*, 2004] and for mantle plumes [*Montelli et al.*, 2004]. We focus on the Pacific plate for three reasons: (1) The effect of sediments on corrected seafloor topography in the Pacific is much smaller than for other regions (e.g., Atlantic) [e.g., *Hillier and Watts*, 2005]. (2) The recently available seismic model for the Pacific upper mantle [*Ritzwoller et al.*, 2004] opens the possibilities to distinguish the effects of the deep mantle plumes and the shallow upper mantle structure on seafloor topography. (3) Plate motions may affect the onset of SSC via non-Newtonian rheology [*van Hunen et al.*, 2005] and hence lithospheric evolution. This may contribute to some of the regional differences in depth-age relations as observed by *Marty and Cazenave* [1989]. The uniform plate motion and tectonics for a single plate (i.e., the Pacific plate) minimizes such regional effects.

[10] This study is motivated by a number of recent developments in data compilation, topography analyses, seismic tomography, and mantle dynamics:

[11] 1. Recently available data sets including high-resolution bathymetry [*Smith and Sandwell*, 1997], seamounts distribution [*Wessel*, 2001], LIPs [*Coffin and Eldholm*, 1994], and sediment thickness [*National Geophysics Data Center* (*NGDC*), 2003] make it possible to significantly improve the topography analyses over previous work [*Heestand and Crough*, 1981; *Schroeder*, 1984; *Marty and Cazenave*, 1989; *Carlson and Johnson*, 1994; *Stein and Stein*, 1992; *Davies and Pribac*, 1993; *Panasyuk and Hager*, 2000].

[12] 2. Recent seismic studies provide better constraints on deep mantle plumes [*Montelli et al.*, 2004; *Ritsema et al.*, 1999] and the shallow mantle and lithospheric structures [*Ritzwoller et al.*, 2004]. Particularly, the latter study with a thermal parameterization in the seismic inversion shows that the Pacific lithosphere older than 70 Ma is warmer than predicted from the HSC model, and that the inverted lithospheric structure is consistent with what may result from SSC [*van Hunen et al.*, 2005]. It is important to examine the implications of these seismic structures for seafloor topography.

[13] 3. Recent dynamic modeling of SSC by *Huang and Zhong* [2005] confirmed the cooling effects of SSC on the underlying mantle and surface topography, first suggested by *O'Connell and Hager* [1980]. However, *Huang and Zhong* [2005] also demonstrated that SSC in a mantle with significant internal heating can indeed lead to thermal structure for the mantle and lithosphere that is required for the plate model, suggesting that the plate model is dynamically viable.

[14] 4. Recent topography analyses by *Hillier and Watts* [2004, 2005] for the Pacific with a regional-residual separation method, MiMIC, to remove the effects of seamounts and LIPs show that the plate model remains necessary for seafloor

older than 85 Ma and that at younger seafloor the topography follows a HSC model but with 10% slower subsidence rate than the previous HSC models. Recently, *Crosby et al.* [2006], by analyzing gravity and topography in different oceans, also suggested the need for a plate model. These results need independent check using different methods.

[15] This paper is organized as follows. Section 2 describes the procedures in removing and correcting sediments, seamounts and LIPs from the seafloor topography and presents the corrected topography. Section 3 analyzes the depth-age relation and its implications for the HSC and plate models. Section 4 presents the residual topography from different reference models (HSC and plate) and correlates the topography with seismic models. Sections 5 and 6 present discussions and conclusions.

2. Removal of Sediments, Seamounts, and LIPs and Corrected Topography

[16] Our topography correction scheme starts with removal of the effects of sediments from a bathymetry data set [*Smith and Sandwell*, 1997] on a $0.1^\circ \times 0.1^\circ$ grid (resampled). The bathymetry at this resolution is sufficient for this type of topography analyses [e.g., *Hillier and Watts*, 2005]. The sediment data set is obtained from *NGDC* [2003]. Following *Carlson and Johnson* [1994], we employ the following equation to remove the effects of sediments:

$$d_c = d_o - 0.22h - 1.4 \times 10^{-4} h^2, \quad (1)$$

where h, d_o, and d_c are the sediment thickness, the original and corrected topography all in meters, respectively. This correction is generally small except in some equatorial regions of the Pacific, and the resulting corrected topography is shown in Figure 1a. On the basis of this topography, we will apply further corrections for seamounts, oceanic islands, and LIPs.

2.1. Removal of Seamounts and LIPs

[17] Recently, *Wessel* [2001] determined the size (i.e., base radius and height) and location of seamounts from gravity observations. In his published data set, there are more than 8000 seamounts with heights > 1 km in the Pacific, and most of these are located at low latitudes and in the western Pacific (Figure 1b). We remove the effects of seamounts on topography by excluding a certain region surrounding each seamount from further analysis. The excluded region for each seamount is circular in shape with a radius that is 1, 2, or 3 times of the base radius of the seamount, for which we denote as R_s = 1, 2 and 3, respectively. Seamounts and oceanic islands are often surrounded by sediment refills and are underlain by a thickened crust [*ten Brink and Brocher*, 1987; *Caress et al.*, 1995; *Leahy and Park*, 2005]. Using $R_s > 1$ helps reduce the effects of the sediment refills and thickened crust on topography analyses. The practice that the topography data near seamounts are not considered in topography analyses is similar to that in the work of *Schroeder* [1984]. However, the current study uses a much improved seamount data set [*Wessel*, 2001]. Our method is different from the regional-residual separation method used by *Hillier and Watts* [2004, 2005] in that they attempt to reconstruct the topography in areas occupied by seamounts, oceanic islands, and LIPs. The topography with seamounts removed is shown in Figure 1b with excluded regions that are 3 times the base radius for each seamount (i.e., R_s = 3). The effects of different values of R_s will be discussed later.

[18] We use the similar approach to further exclude LIPs and the resulting topography is shown in Figure 1c. The data set for LIPs is taken from *Coffin and Eldholm* [1994]. In this data set the boundaries of LIPs are given, and we only exclude the regions bounded by the LIP boundaries. Slight modifications are made to the LIP data set to include parts of the Marshall-Gilbert Seamounts and the Magellan Rise as LIPs. The LIP data set includes topography anomalies of relatively large horizontal extent, but it also includes features of seamount size. Consequently, there are overlaps between the LIP and seamount data sets. The excluded regions in Figure 1c represent the union of these two data sets.

2.2. Regions Affected by Seamounts and LIPs

[19] Before performing age-topography analyses, we first analyze how much area is excluded owing to the removal of the seamounts and LIPs and how the excluded area is distributed geographically and with regard to the seafloor age. The age of the seafloor is taken from *Müller et al.* [1997] (Figure 1d). We only analyze regions within the Pacific plate but excluding trench and outer rise regions (Figure 1c) [e.g., *Hillier and Watts*, 2005]. We also limit our analysis to regions where a seafloor age is assigned by *Müller et al.* [1997]. We compute the area in each 2 Ma age bin for seafloor up to 166 Ma before and after the removal of seamounts and LIPs (Figures 1a–1c). Before any removal, seafloor younger than ~50 Ma generally occupies more area than older seafloor except near ~112 Ma where the area is significantly larger (Figure 2a). The removal of seamounts with R_s = 3 excludes a significant area of seafloor for all ages, particularly for seafloor older than 80 Ma (Figure 2a), suggesting that older seafloor is affected more by seamounts [*Wessel*, 2001]. For example, for seafloor older than 155 Ma more than 50% of seafloor area is excluded because of its proximity to seamounts (Figure 2a). Further removal of LIPs only affects seafloor older than ~130 Ma. After the removal of seamounts and LIPs, more than 50% of seafloor older than 140 Ma is excluded (Figure 2a).

[20] Seamounts and LIPs are not uniformly distributed in the Pacific. The number of seamounts and LIPs north and northeast of the Hawaiian island chain is significantly less than that in the south until ~30°S (Figure 1c). This motivates us to divide the Pacific plate into three regions as marked in Figure 1c in our topography analyses: the northern, central, and southern regions. Both the northern and southern regions have significantly fewer seamounts and LIPs, while the central region includes the Hawaiian swell, the South Pacific super-swell and the Darwin Rise with densely populated seamounts and LIPs (Figure 1c). Figures 2b–2d show how much seafloor area is affected by the removal of seamounts with R_s = 3 and LIPs, for the northern, central, and southern regions, respectively. While the removal does not significantly affect the northern and southern regions, it greatly reduces the area of the central region for topography analyses, particular for seafloor older than 90 Ma, consistent with seamount and LIP distributions in these regions (Figure 1c). The oldest seafloor is ~135 Ma

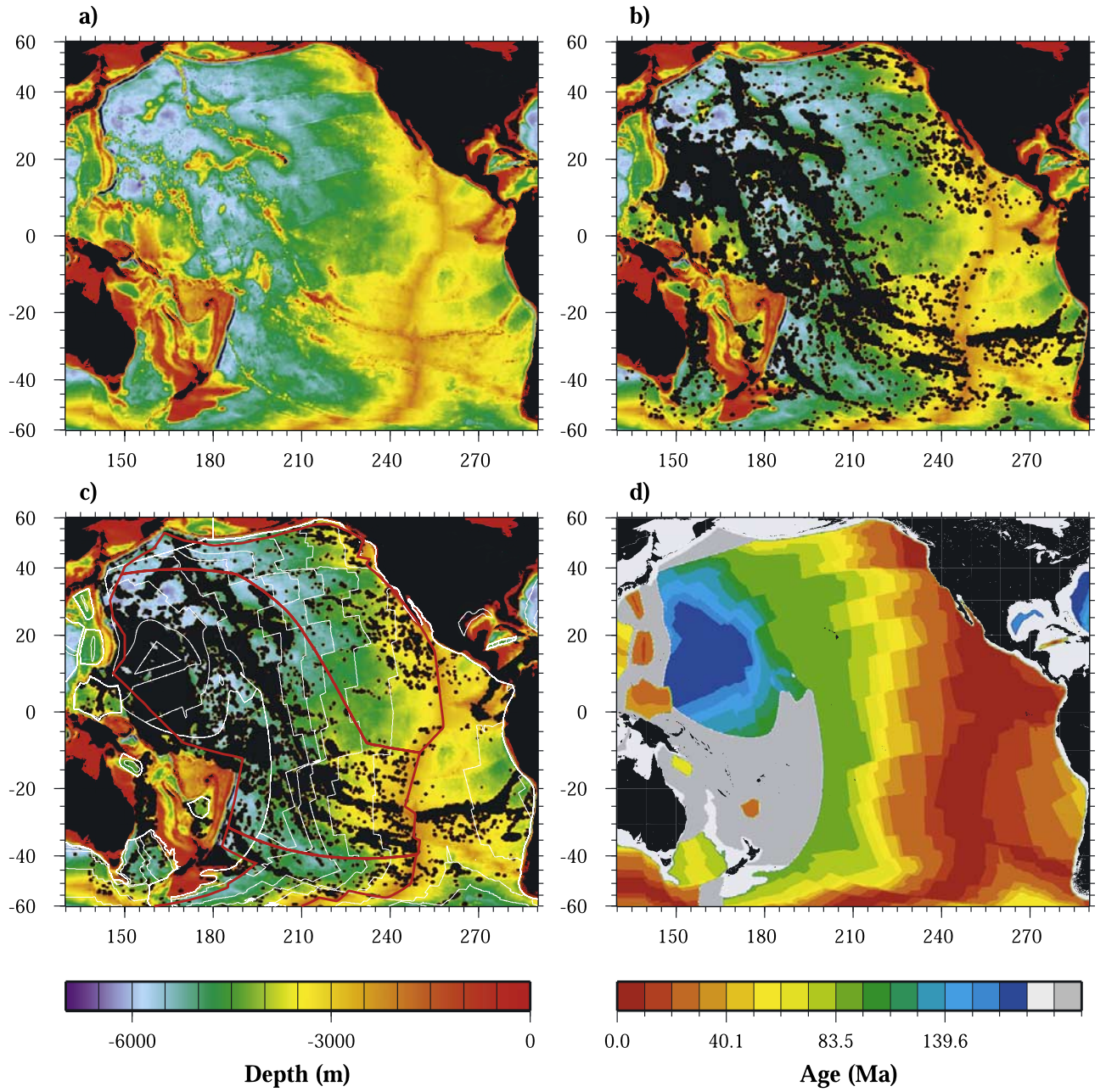

Figure 1. Topographic maps for the Pacific with corrections for (a) sediments, (b) sediments and seamounts, (c) sediments, seamounts, and large igneous provinces (LIPs), and (d) the seafloor age map. The black regions in Figures 1a–1c are either above sea level or for seamounts and LIPs. The thick red lines in Figure 1c define the northern, central, and southern Pacific regions. The thin white lines in Figure 1c represent contours of seafloor age in increments of 20 Ma. The Behrman projection is used.

and ~110 Ma in the northern and southern regions, respectively (Figures 2b and 2d), and the central region is limited to 166 Ma (Figure 2c). Both the northern and southern regions have relatively small but still significant area for seafloor older than 80 Ma.

3. Topography and Depth-Age Relation

3.1. Topography Prior to Removal of Seamounts and LIPs

[21] We begin analysis by examining the original topography before any removal of seamounts and LIPs (i.e., Figure 1a). Many of the previous topography analyses were done to bathymetry data sets that included seamounts and LIPs [e.g., *Stein and Stein*, 1992; *Smith and Sandwell*, 1997]. Consequently, sophisticated statistics with medians and modes were needed in these studies [e.g., *Carlson and Johnson*, 1994]. By correcting for sediments and removing outliers like seamounts and LIPs, we can employ relatively simple statistical approaches and perform topography analyses in normal seafloor areas.

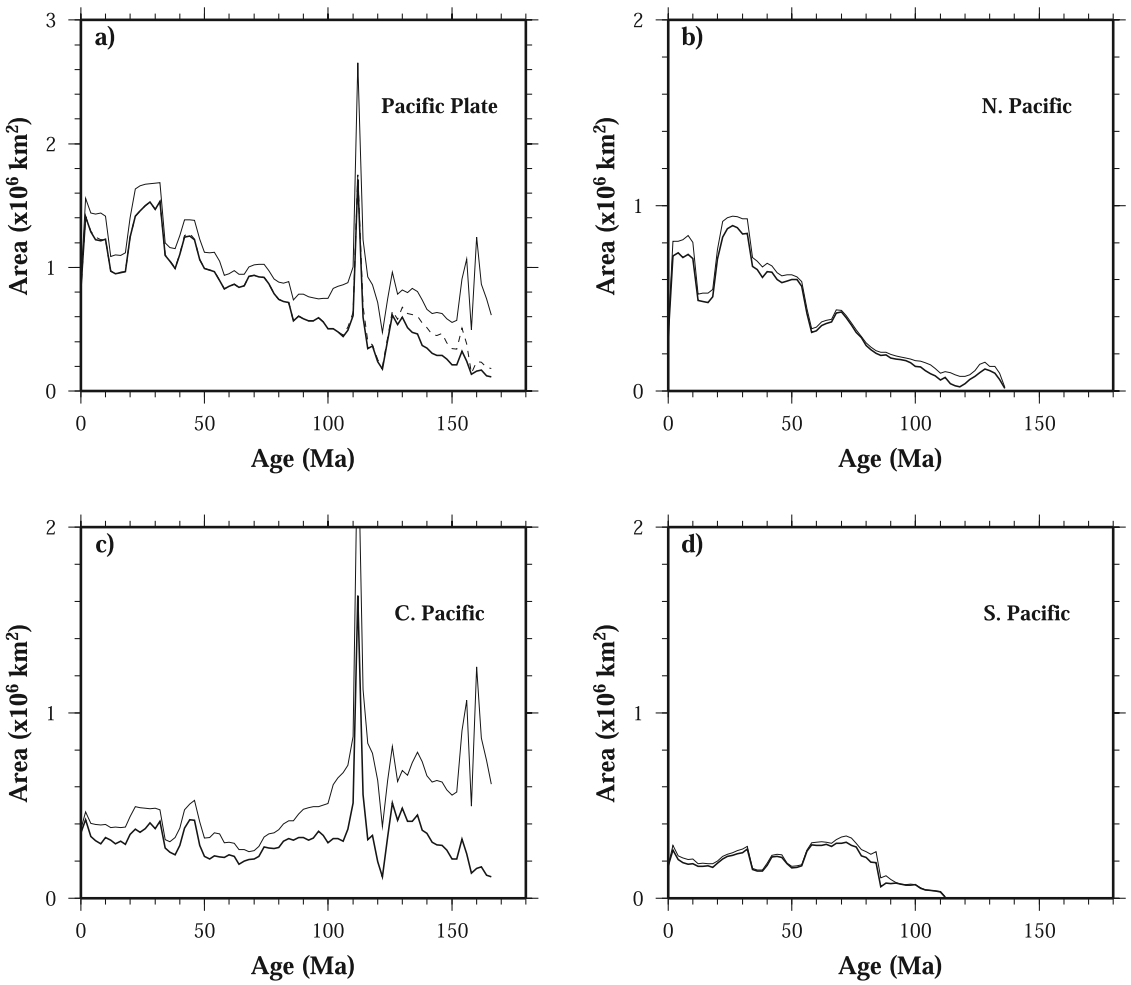

Figure 2. Area of seafloor in 2 Ma age bin versus seafloor age for (a) the Pacific plate, (b) the northern region, (c) the central region, and (d) the southern region before (thin solid lines) and after removal of seamounts and LIPs (thick solid lines). In Figure 2a the dashed line represents the area after the removal of seamounts only.

[22] We compute area-weighted mean ocean depth and its standard deviations for each 2 Ma age bin centered at age i as

$$d_{mean} = \int_{i-1<age<i+1} d\cos\theta d\theta d\phi \Big/ \int_{i-1<age<i+1} \cos\theta d\theta d\phi, \quad (2)$$

$$\sigma = \left[\int_{i-1<age<i+1} (d - d_{mean})^2 \cos\theta d\theta d\phi \Big/ \int_{i-1<age<i+1} \cos\theta d\theta d\phi \right]^{1/2}, \quad (3)$$

where the age, i, and 1 are in Ma. The mean ocean depth and its standard deviation versus lithospheric age for the whole Pacific plate, and the northern, central, and southern regions are shown in Figures 3a, 3b, 3c, and 3d, respectively. There are two important features in the results for the Pacific plate as a whole. First, the topography stops deepening with age at ~70 Ma (i.e., topographic "flattening" which is used to refer the reduced topographic subsidence with seafloor age). Second, the standard deviations are nonuniform and are much larger (>1 km) for seafloor older than ~70 Ma (Figure 3a). If the topography is examined region by region, then it is clear that these features are largely controlled by the central region. For the northern region, it appears that the "flattening" does not start until ~85 Ma, and the standard deviation is uniformly small (generally < ~400 m) also until ~85 Ma where it starts to increase significantly (Figure 3b). The central region (Figure 3c) displays similar features as those for the whole Pacific plate, in particular the large standard deviations (Figure 3c). The southern region also shows a reduced topographic deepening with age at ~70 Ma and relatively large standard deviations for old seafloor (Figure 3d). Similar plots for unprocessed Pacific topography can be found in previous studies [e.g., *Renkin and Sclater*, 1988].

[23] Two features deserve further discussion. First, significant variations in mid-ocean ridge (MOR) topography exist in the Pacific, as previously reported by *Marty and Cazenave* [1989] and *Davies and Pribac* [1993]. The mean MOR topography is ~−3100 m, −2900 m and −2700 m, in the northern, central, and southern regions, respectively (Figures 3b–3d). The topography along the MOR shows a sudden change at ~24°S at the Easter microplate, and this

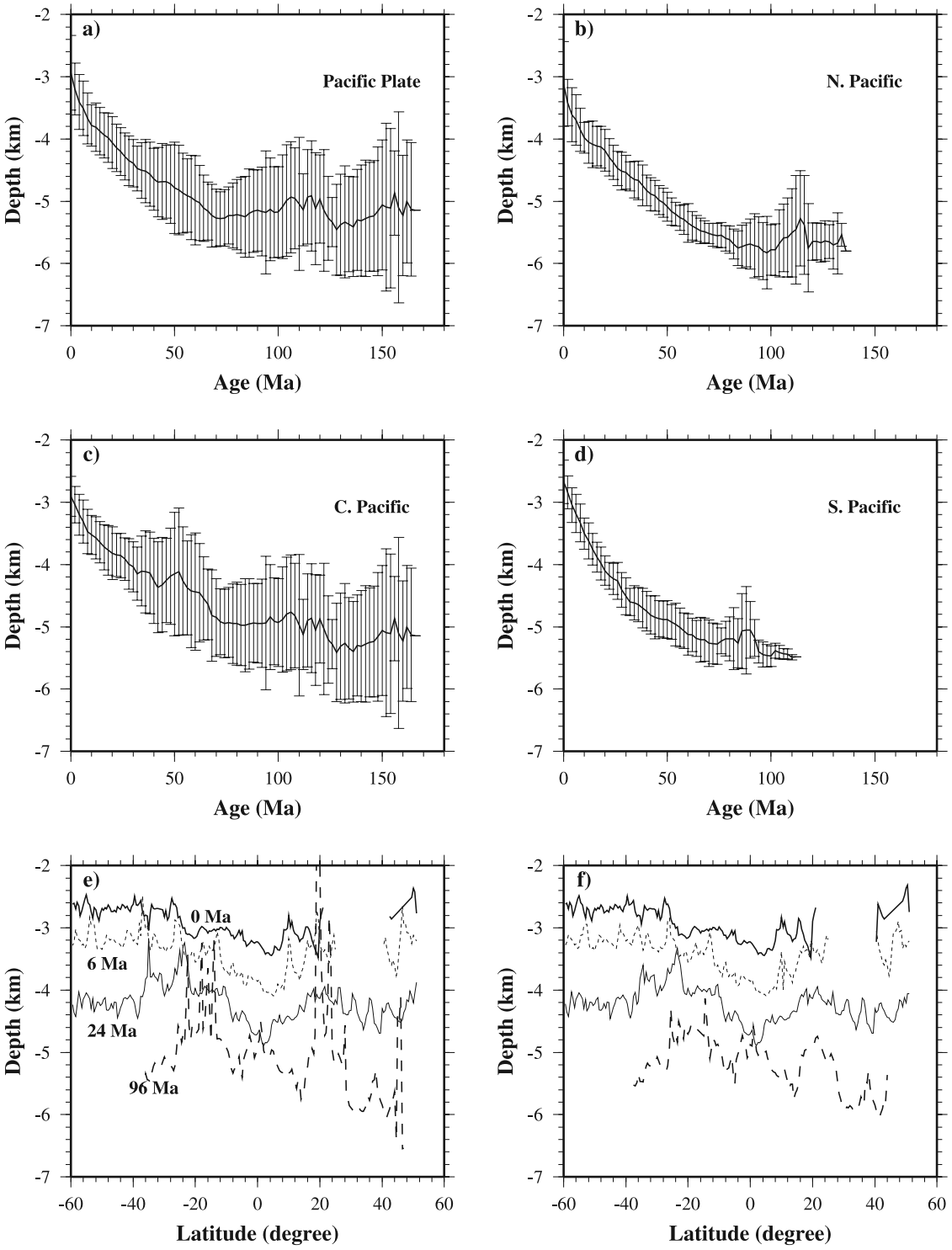

Figure 3. Mean depths and standard deviations in 2 Ma age bins versus seafloor age for (a) the Pacific plate, (b) the northern Pacific region, (c) the central Pacific region, and (d) the southern Pacific region for the topography corrected only for sediments, as well as topography profiles versus latitude for four different ages (0, thick solid line; 6 Ma, thin dashed line; 24 Ma, thin solid line; and 96 Ma, thick dashed line) (e) before the removal of seamounts and LIPs and (f) after the removal of seamounts and LIPs.

can still be seen along the 6 Ma old seafloor profile (Figure 3e for latitudinal dependence of topography averaged over 0.5° in latitude for seafloor ages: 0, 6, 24, and 96 Ma). Additionally, it is clear from the 96 Ma profile that the seamounts cause large variations in topography that are not seen for relatively young seafloor. Second, the standard deviation in topography seen in Figures 3a–3d is generally much smaller at young seafloor than at old seafloor. Although this may reflect the fact that younger seafloor with a thinner elastic plate can only support seamounts with

smaller sizes [*Wessel*, 2001], we believe that this is more likely because the topographic variations at young and old seafloors are caused by different mechanisms. Specifically, the variations at old seafloor are controlled by seamounts and LIPs, while they do not significantly affect topographic variations at young seafloor (Figure 3e).

3.2. Corrected Topography

[24] Because seamounts and LIPs cause significant topographic variations at various length scales, it is important to eliminate their effects in order to use topography to constrain dynamic models of the mantle and lithosphere. The removal of seamounts alone with R_s = 3 significantly deepens the mean depths for 40–125 Ma seafloor for the Pacific plate, while leaving younger seafloor almost unchanged (solid line in Figure 4a). The standard deviations are also reduced significantly between 40 and 125 Ma, but large topographic variations remain for older seafloor (thick error bars in Figure 4a). Further removal of LIPs primarily affects the topography for seafloor older than 125 Ma by significantly deepening the topography and reducing the topographic variations (solid line and error bars in Figure 4b).

[25] For the whole Pacific plate, the topography corrected for seamounts and LIPs shows a "flattening" at 70 Ma that continues until ~115 Ma and then deepens (solid line in Figure 4c), different from that for the original topography (Figures 3a and thin line in Figure 4c). More importantly, the corrected topography has nearly uniform standard deviations for all ages, because removal of seamounts and LIPs greatly reduces the topographic variations at old seafloor (Figure 4c). We consider the uniform standard deviations for all ages as an important indication that the effects of seamounts and LIPs are effectively eliminated and that the remaining variations in topography are caused by other processes. The choice of R_s has only a small effect on the corrected topography especially when R_s is greater than 1. The mean ocean depths with R_s = 2 are only slightly shallower than that for R_s = 3 (dashed line in Figure 4c). The differences in mean depths between R_s = 1 and R_s = 2 cases are slightly larger than those between R_s = 2 and R_s = 3. Similar results are seen on regional scales (Figures 4d–4f for R_s = 3). The latitudinal dependence of the corrected topography for different seafloor ages confirms that the corrections mainly affect the relatively old seafloor (Figures 3e and 3f). It also shows rapid changes in topography across some fracture zones (at ~20°S and −8°S of the 24 Ma profile in Figure 3f) and gradual variations such as the Hawaiian swell (at ~20°N of the 96 Ma profile).

3.3. Mean Depth Versus Seafloor Age

[26] The topography in the northern region may better constrain models of lithospheric thermal structure, because the region is significantly less affected by seamounts, LIPs and mantle plume activities [*Davies*, 1988a; *Sleep*, 1990; *Montelli et al.*, 2004]. We first compare the mean depths from the northern region with two HSC models: CJ from *Carlson and Johnson* [1994] and HW HSC from *Hillier and Watts* [2005]. Model CJ was derived from basement depths of a number of drilling sites in global oceans. The topography in Model CJ is given by $d = d_0 - 345t^{1/2}$, where t is lithospheric age in Ma and d_0 is the MOR topography, similar to that in the work of *Parsons and Sclater* [1977]. Model HW HSC was derived from filtered topography in the North Pacific Ocean (i.e., the entire Pacific north of the equator) using the MiMIC algorithm. In models by *Hillier and Watts* [2005], the topography varies as $d = d_0 - 307t^{1/2}$ for t < 85 Ma (i.e., a HSC model with a slower subsidence rate), but for older seafloor it varies as $3010\exp(-0.026t)$, similar to the plate models in the work of *Parsons and Sclater* [1977] and *Stein and Stein* [1992].

[27] If the MOR topography d_0 for the HSC models is chosen to be −2950 m, model HW HSC fits well the mean depths for the northern region for seafloor younger than ~85 Ma and the fit is better than model CJ (Figure 5a). For seafloor older than 85 Ma, both models HW HSC and CJ overpredict the depth. However, we found that model HW HSC-Plate (note that HW HSC-Plate is the same as HW HSC for t < 85 Ma but is the plate model for t > 85 Ma) fits the topography for seafloor older than 85 Ma in the northern region reasonably well (Figure 5a). This is interesting because model HW HSC-Plate was derived from the topography processed with a completely different approach for a much larger region with many more seamounts and LIPs than the northern region in this study. Compared with model HW HSC-Plate, the GDH1 model of *Stein and Stein* [1992] gives a larger depth for young seafloor, but the overall topographic variations from the MOR to 166 Ma are similar. It should be pointed out that all the HSC and plate models considered here use d_0 = −2950 m. This MOR topography provides a better fit to the northern region topography (Figure 5a), although it is slightly higher than that in the original form of model HW HSC-Plate (−3010 m) and for the northern region (−3126 m).

[28] The MOR topography for the southern region is ~400 m shallower than that for the northern region. This ~400 m difference between these two regions seems to exist for nearly all ages, as shown by the fine dashed line in Figure 5b for the southern region in which the topography is shifted down by 400 m for all ages. Although the topographic "flattening" for the southern region starts at ~70 Ma, or 15 Ma earlier than in the northern region, the southern region is still reasonably well fit with model HW HSC-Plate. This suggests that model HW HSC-Plate provides an accurate description of seafloor topography for seafloor that is not significantly affected by seamounts, LIPs, and plumes. We also plotted the mean depths for the central region and entire Pacific plate in Figure 5b, shifting the curves by 0.3 km and 0.2 km, respectively, such that the depths are similar at young ages to that for the northern and southern regions. The central region is clearly anomalous with much smaller depths than other two regions between 50 Ma and 110 Ma (thin dashed line in Figure 5b). The mean depths for the whole Pacific plate follows model HW HSC-Plate before the topographic "flattening" at ~70 Ma, and the topography deepens again after 110 Ma and oscillates around model HW HSC-Plate (thick dashed line in Figure 5b).

4. Residual Topography and Correlations With Seismic Models

[29] Seafloor topography reflects the integrated effects of the mantle and lithosphere. The age and geographical dependences of seafloor topography provide important constraints on lithospheric thermal structure and mantle

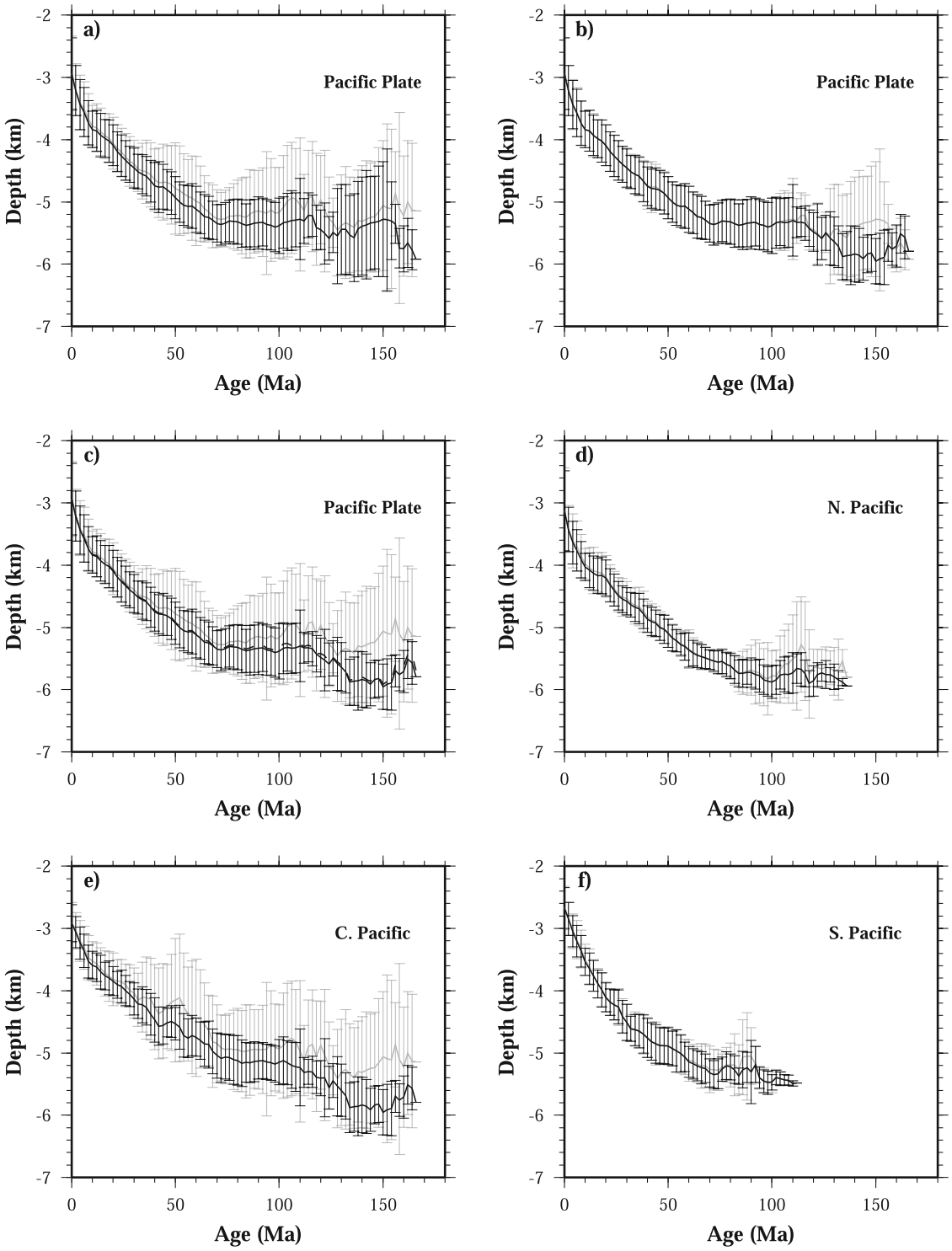

Figure 4. Mean depths and standard deviations in 2 Ma age bins versus seafloor age for the entire Pacific plate (a) before (thin lines) and after (solid lines) removal of seamounts only, (b) before (thin lines) and after (solid lines) further removal of LIPs, and (c) before (thin lines) and after (solid lines) removal of seamounts and LIPs and for different R_s = 2 (dashed line), and for (d) the northern Pacific region, (e) the central Pacific region, and (f) the southern Pacific region for the topography before (thin lines) and after (solid lines) removal of seamounts and LIPs. R_s = 3 for all except for the dashed line in Figure 4c.

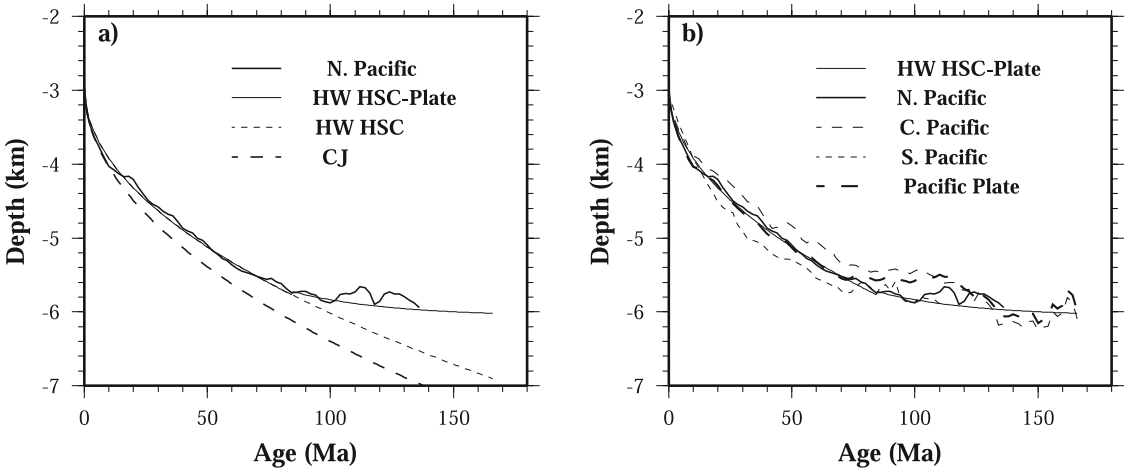

Figure 5. Mean depths in 2 Ma age bins versus seafloor age (a) for the northern region (thick solid line), the HSC-Plate model (thin solid line), and HSC model (thin dashed line) from *Hillier and Watts* [2005] and the HSC from *Carlson and Johnson* [1994] (thick dashed line), and (b) for the HSC-Plate model from *Hillier and Watts* [2005] (thin solid line), the northern region (thick solid line), the central region (thin dashed line), the southern region (fine dashed line), and the entire Pacific plate (thick dashed line). In Figure 5b, the curves for the southern and central regions and the Pacific plate are shifted down by 0.4, 0.3, and 0.2 km, respectively.

dynamics. Separating lithospheric and mantle contributions to the topography helps deduce the dynamics of the mantle [*Davies and Pribac*, 1993; *Panasyuk and Hager*, 2000]. Lithospheric contributions can be estimated from the HSC or plate models that are constructed from seafloor topography data [e.g., *Parsons and Sclater*, 1977; *Stein and Stein*, 1992; *Carlson and Johnson*, 1994; *Hillier and Watts*, 2005], and they may also be inferred from seismic models of lithosphere such as that in the work of *Ritzwoller et al.* [2004].

4.1. Residual Topography With Respect to HSC and Plate Models

[30] We will first use the depth-age relations from models HW HSC, HW HSC-Plate and CJ to determine the lithospheric contribution to the topography and construct the residual topography that can be used to constrain the mantle contribution. Model HW HSC-Plate fits well the mean depths in the northern region of this study as was discussed earlier (Figure 5a). We assume $d_0 = -2745$ m in model HW HSC and HW HSC-Plate, which leads to zero mean residual topography between 0 and 1 Ma age bin for the entire Pacific plate. The residual topography is computed by subtracting the predicted topography from models HW HSC and HW HSC-Plate from the corrected topography in Figure 1c, similar to that of *Davies and Pribac* [1993] and *Panasyuk and Hager* [2000]. Note that for model HW HSC, we use $d = -2745 - 307t^{1/2}$ for all seafloor ages.

[31] Residual topographies with respect to the HSC and HSC-Plate models of *Hillier and Watts* [2005] are shown in Figures 6a and 6b, respectively. These residual topographies differ only for seafloor older than 85 Ma. The residual topography at the MOR is positive south of the Easter Island microplate but is largely negative or near zero in the north, reflecting topographic variations along the MOR, as discussed in section 3.1. A large area of the northern region generally shows negative or near zero residual topography in both residual maps. This is caused by the shallower MOR topography used in the depth-age relations than the actual MOR topography for the northern region. The main difference between the two residual maps is in the western Pacific where the residual topography is on average between 600 m and 1000 m with the HW HSC reference model (Figure 6a), but is near zero with the HW HSC-Plate reference model (Figure 6b). This is more clearly demonstrated in Figure 7a that shows the mean residual topography for different age bins for the Pacific. The mean residual topography with the HSC reference model is >600 m for seafloor older than 110 Ma and is significantly larger than standard deviations of topography of <300 m. This difference is significantly larger if the HSC model CJ [*Carlson and Johnson*, 1994] is used as the reference (Figure 7a). Notice that the choice of reference model does not affect the standard deviations.

[32] The residual topography with the HW HSC-Plate reference model clearly shows the Hawaiian swell topography (Figures 6b and 7b). Another prominent topographic high is the South Pacific super-swell located east of Tonga that has a significantly larger horizontal scale than the Hawaiian swell (Figures 6b and 7b). In fact, these two swells are largely responsible for the elevated topography between 80 Ma and 130 Ma in the depth-age curve for the Pacific (Figure 5b) and for the increased residual topography in the same age band (Figure 7a). Other topographic highs are all at the margins of LIPs or densely populated seamounts (e.g., Marshall-Gilbert Seamounts and Megellan Rise) and may be of little dynamic significance. Interestingly, a large area of the Darwin Rise (note that the Darwin Rise which was first proposed by *Menard* [1964] is depicted in Figure 6b, following *McNutt* [1998]), particularly its northern portion, after exclusion of seamounts and LIPs, does not show any positive residual topography with the HW HSC-Plate reference model (Figure 6b). However, with the HW HSC reference model, all the old seafloor including the Darwin Rise shows significant positive residual topography (Figures 6a and 7a).

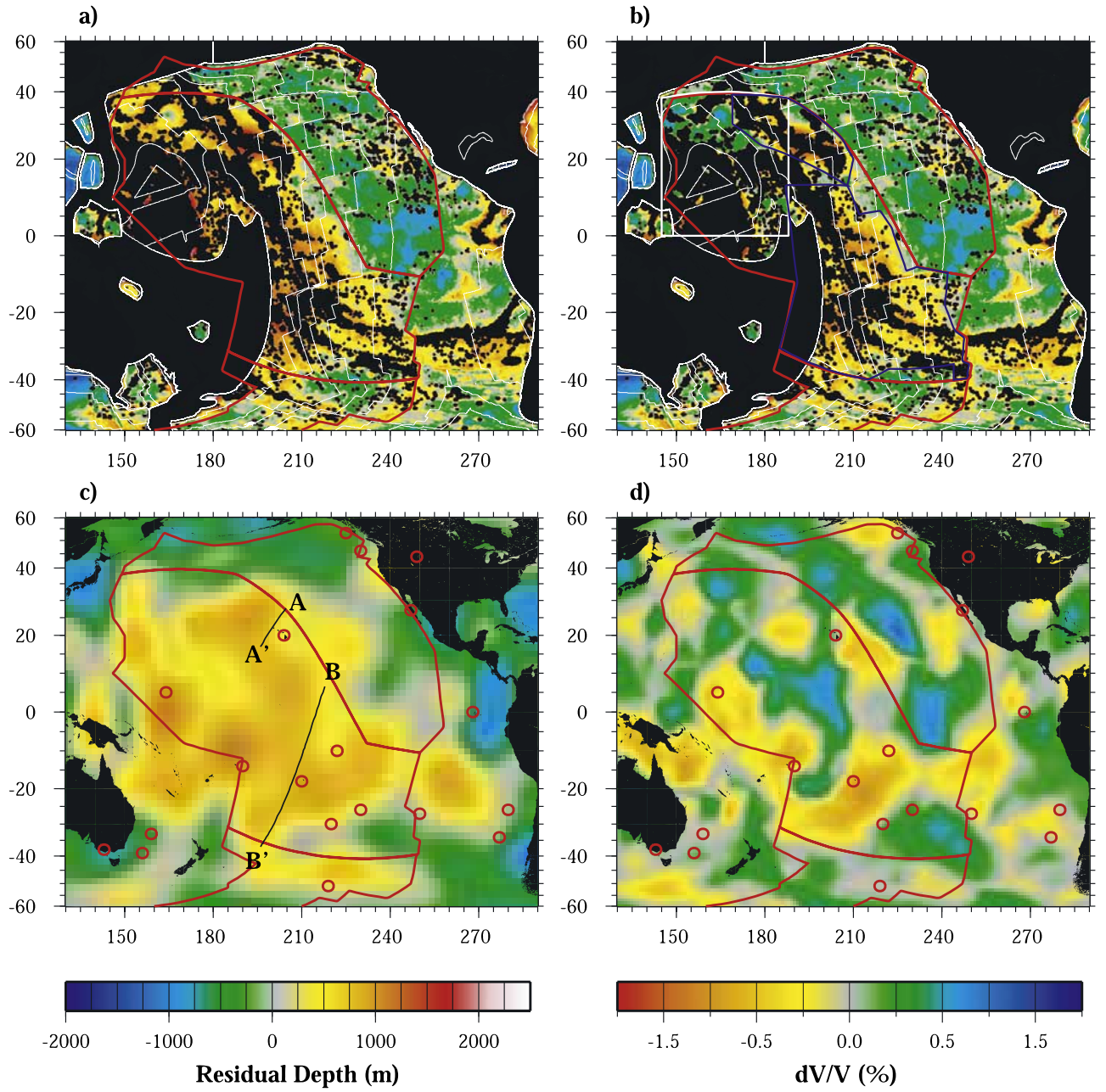

Figure 6. Residual topography maps for the Pacific with respect to (a) the HSC model and (b) the HSC-Plate model of *Hillier and Watts* [2005], as well as seismic velocity anomalies at 2300 km depth from (c) *Ritsema et al.* [1999] and (d) *Montelli et al.* [2006]. The thick red lines in Figures 6a–6d show the northern, central, and southern Pacific regions, and the thin white lines in Figures 6a and 6b represent contours of seafloor age in increments of 20 Ma. In Figure 6b the thick white lines represent the boundaries of the Darwin Rise region [*McNutt*, 1998], and the blue lines mark the Hawaiian swell and South Pacific super-swell regions. In Figures 6c and 6d, red circles represent hotspots. In Figure 6c, black lines are for profiles AA' and BB'. The Behrman projection is used.

4.2. Estimated Topography From a Seismic Model of the Pacific Lithosphere

[33] We now estimate the lithospheric contribution to the topography from *Ritzwoller et al.*'s [2004] recent seismic structure for the Pacific lithosphere. In their inversion of shallow oceanic mantle structure from surface wave data, *Ritzwoller et al.* [2004] parameterized lithospheric structure in terms of apparent thermal age, assuming that the lithospheric thermal structure is governed by a HSC model and that seismic structure can be related to thermal structure via mineral physics and thermodynamics relations [*Shapiro and Ritzwoller*, 2004]. It was found that the inverted apparent thermal age on average is smaller than actual seafloor age for seafloor older than 70 Ma [*Ritzwoller et al.*, 2004] (Figure 8a). The reduced apparent thermal age at relatively old seafloor has been interpreted as a result of lithospheric

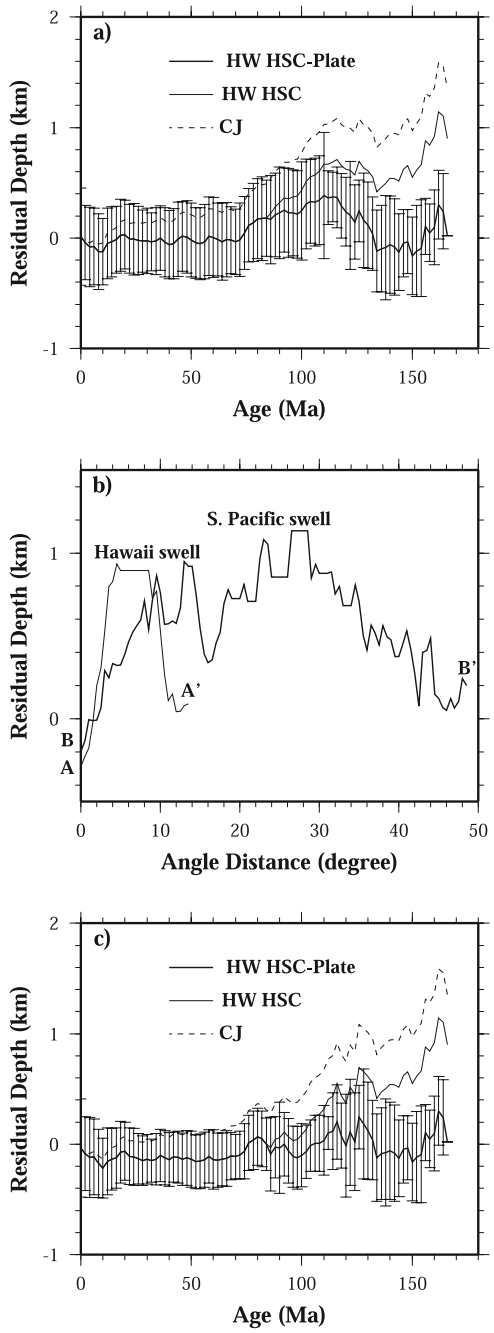

Figure 7. (a) Mean residual depth in 2 Ma age bins versus seafloor age for residual depth for the Pacific plate with respect to the HSC-Plate model by *Hillier and Watts* [2005] (thick solid line) and HSC models by *Hillier and Watts* [2005] (thin solid line) and by *Carlson and Johnson* [1994] (thin dashed line), (b) residual depth profiles AA' and BB' across the Hawaiian swell and South Pacific super-swell as marked in Figure 6c, respectively, and (c) the same as in Figure 7a except that the Hawaiian swell and South Pacific super-swell regions are excluded. In Figures 7a and 7c, standard deviations of residual topography are also shown, and the standard deviations are the same for different reference models and the same as those for the topography in Figure 4c. In Figure 7b the flat tops represent regions occupied by oceanic islands and seamounts.

reheating induced by sublithospheric small-scale convection [*Ritzwoller et al.*, 2004; *van Hunen et al.*, 2005].

[34] We may estimate the topography from the apparent thermal age using a depth-age relation. Here we use the HSC depth-age relation from model HW HSC (i.e., $d = -2745 - 307t^{1/2}$), the same as that used earlier for computing the residual topography. The estimated topography shows elevated topography at the MOR and deepens with seafloor age, as expected (Figures 8b and 1c). In Figures 9a–9c the estimated topography is compared with the corrected topography along three profiles CC', DD', and EE'. Although the seismic model has a limited horizontal resolution (~1000 km) and is hence necessarily smooth, these profiles show reasonable agreement between the estimated and corrected topographies, even for topographic variations across fracture zones (Figure 9a for the Mendocino fracture zone at ~40°N). The depth-age relation for the estimated topography also shows a good agreement with that for the corrected topography, including the "flattening" at ~70 Ma and then continuous deepening at ~120 Ma (Figure 9d). The estimated topography shows similar standard deviations to the correct topography, except for seafloor older than 140 Ma where the estimated topography displays larger variations (Figure 9d).

[35] However, the estimated topography from the seismic model also differs from the observed corrected topography in a number of ways. The averaged topography near the MOR is in general significantly deeper than the corrected topography (Figure 9d). This is evident in the topography profiles in Figures 9b and 9c. Differences also exist in regions off the west coast of the U.S. (Figure 8b) and in some regions with extensive volcanism (e.g., ~210° longitude in Figure 9c). These differences may be caused by regional tectonic features that present difficulties for seismic inversion of lithospheric thermal structure. For example, features like the ocean-continent contrast off the west coast of the US, and thin lithosphere and rapidly varying topography at the MOR all make it difficult to recover accurately the thermal structure of oceanic lithosphere. Thermal structure in regions with extensive volcanisms is also difficult to resolve, because of compositional anomalies.

[36] We construct residual topography with the estimated topography from the seismic model as a reference model (Figure 8c). Compared with the residual topography with reference model HW HSC-Plate (Figure 6b), two features from the seismically derived residual topography deserve discussion. First, the residual topography near the MOR for the North Pacific is mostly positive. This is expected on the basis of the overestimated apparent thermal age or topography in these regions from the seismic model (Figures 8a and 8b). Second, the seismically derived residual topography also shows positive anomalies near the South Pacific super-swell and Hawaiian swell regions, but the area of the swells is much reduced, compared with that from model HW HSC-Plate. Particularly, the mid section of the Hawaiian swell is missing, while an additional positive anomaly emerges at the end of the Hawaiian volcanic chain (Figure 8c).

5. Discussion

[37] The goal of this paper is to understand the deviations of seafloor topography from the HSC model prediction, a

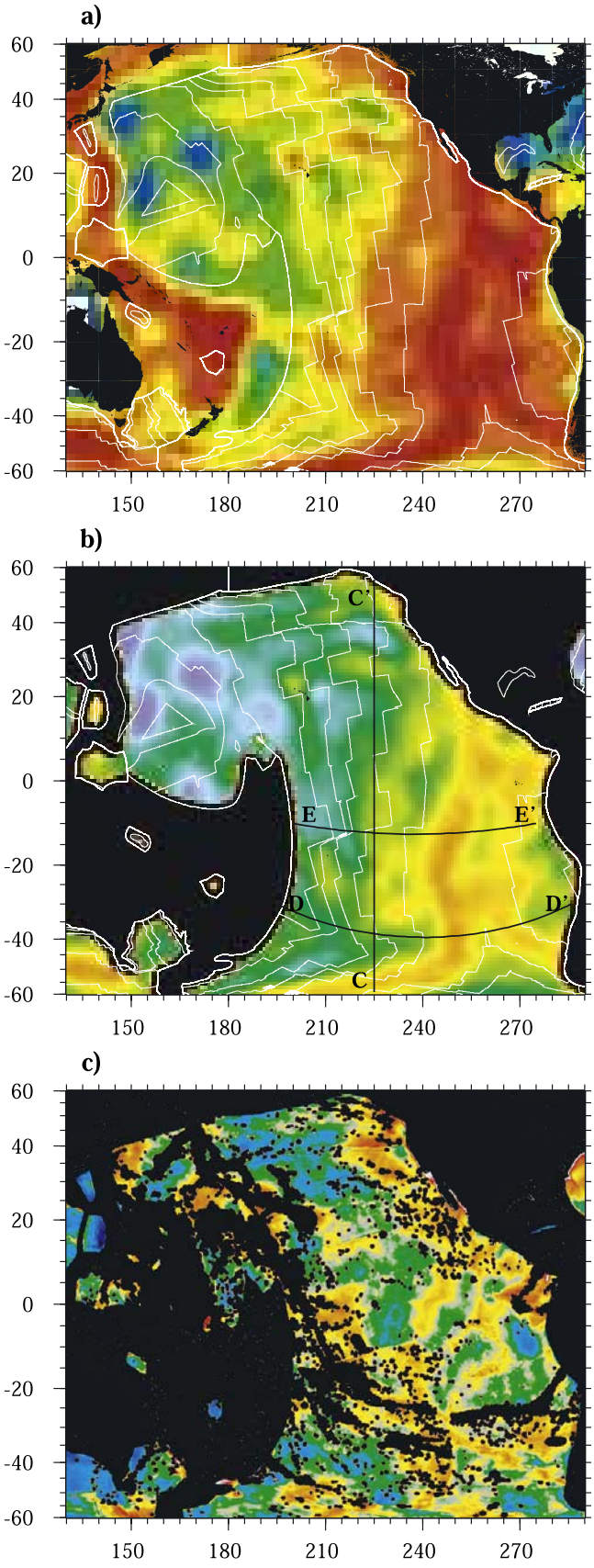

long-standing geophysical question. More specifically, we would like to answer the question whether the deviations are caused by lithospheric reheating derived from sublithospheric small-scale convection (i.e., the plate model) [*Parsons and Sclater*, 1977] or by mantle upwelling plumes [*Davies*, 1999; *McNutt*, 1998], or by some other processes. To resolve this issue, we construct the corrected topography for the Pacific plate by removing sediments, seamounts and LIPs, and perform statistical analyses to the corrected topography.

5.1. Depth-Age Relation for the Pacific Plate

[38] The deviations of topography at the relatively old seafloor from the HSC model prediction remain significant in the Pacific after removal of sediments, seamounts and LIPs, although the removal of these surface features reduces the deviations moderately (Figures 4 and 5). This conclusion holds not only for the entire Pacific plate, but also for three subdivisions of the Pacific: northern, central, and southern Pacific regions (Figure 1c). That the similar deviations of topography exist in the northern region is particularly important, because this region is not directly affected by any known major plumes, suggesting that the reduced topography at old seafloor is a general feature for the Pacific, irrespective of mantle plumes. Our study confirms the basic conclusion from many previous studies on the depth-age relations that did not remove seamounts and LIPs [e.g., *Stein and Stein*, 1992] and is also consistent with a recent study for the North Pacific (i.e., for the entire Pacific Ocean north of the equator, which is a much larger area than the northern region in the current study) by *Hillier and Watts* [2005] using a different filtering scheme to remove the effects of seamounts and LIPs. However, our results are different from *Heestand and Crough* [1981] and *Schroeder* [1984] in which the deviations from the HSC model were suggested to be caused by seamounts, LIPs and plumes. This difference between our conclusions may be due to the more complete seamount and LIPs data sets used in our studies.

[39] Removal of the seamounts and LIPs greatly reduces the variability of seafloor topography and leads to nearly uniform standard deviations in ocean depth of ~300 m for all ages (Figure 4). *Davies and Pribac* [1993] suggested that the topographic variations of hundreds of meters along the MOR (e.g., Figure 3e) may be caused by incomplete homogenized thermal anomalies that are inherent to mantle convection processes. If this mantle process of incomplete homogenized thermal anomalies exists uniformly below oceanic plates of all ages, then this process may help explain the nearly uniform standard deviations of ~300 m.

[40] It is worthwhile to point out that the depth-age relation for the Pacific plate may not necessarily be true

Figure 8. (a) Apparent thermal age for the Pacific from *Ritzwoller et al.* [2004], (b) estimated topography, and (c) residual topography. The thin white lines in Figures 8a and 8b represent contours of seafloor age in increments of 20 Ma. Topographic profiles CC', DD', and EE' are marked in Figure 8b. The color scales for Figures 8a, 8b, and 8c are the same as those for Figures 1d, 1c, and 6a, respectively. The Behrman projection is used.

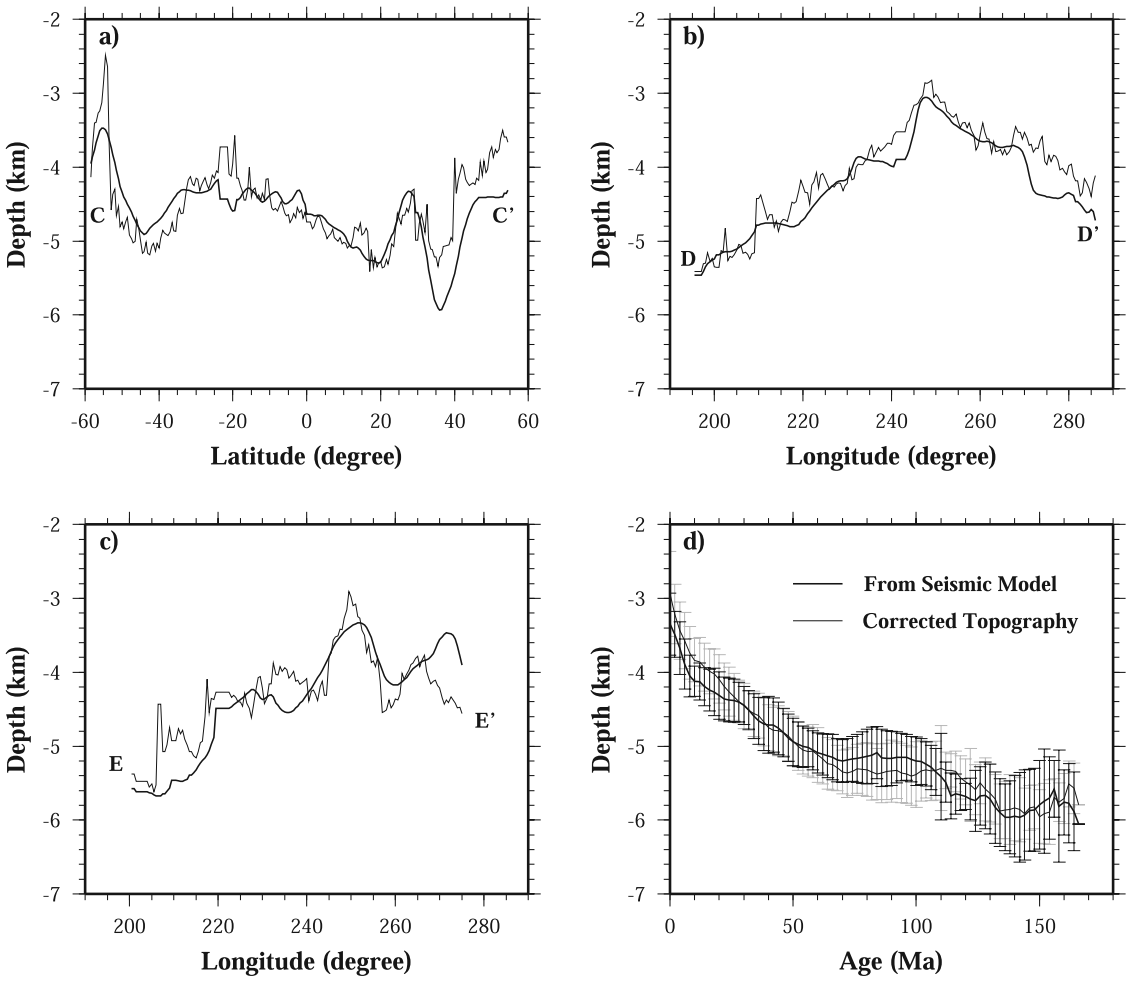

Figure 9. Topographic profiles (a) CC', (b) DD', and (c) EE' as marked in Figure 8b for corrected topography (thin lines) and estimated topography from the seismic model (thick lines), and (d) mean depths and standard deviations in 2 Ma age bins versus seafloor age for the Pacific plate for seismically derived topography (thick solid line and its corresponding error bars) and for corrected topography (thin solid line and its corresponding gray error bars).

for other oceanic plates. *Marty and Cazenave* [1989] reported regional variations in the depth-age relations in which ocean depths for some regions follow the HSC model to much older seafloor age. Regional variations in the depth-age relations may be expected because of regional mantle plume activities and dynamic interaction between the mantle and lithosphere that affect seafloor topography. The latter should depend on plate motion as a result of nonlinear feedback between mantle flow and mantle rheology [e.g., *van Hunen et al.*, 2005]. However, topography analyses for other major oceanic plates are more challenging because of potentially large errors in sediment corrections [e.g., *Carlson and Johnson*, 1994].

5.2. Role of Convective Upwelling Plumes

[41] There is little doubt that convective upwelling plumes produce significant topographic highs that cause deviations from the HSC predictions, as evident by the Hawaiian swell and the South Pacific super-swell (Figure 6b). The locations of the Hawaiian swell and the South Pacific super-swell generally correlate with seismically slow anomalies in the lower mantle (Figures 6c and 6d) [*Ritsema et al.*, 1999; *Montelli et al.*, 2006], although it remains a great challenge to image seismically mantle plumes, especially in the upper mantle where mantle plumes are expected to be much thinner owing to the small viscosity there. For example, the Hawaiian plume is constrained to be <70 km in radius from the vertical motion history of Hawaiian Islands [*Zhong and Watts*, 2002]. It should be pointed out that the swell topography is largely caused by plume materials that spread out below the lithosphere rather than by plume conduits [*Davies*, 1988a; *Sleep*, 1990; *Olson*, 1990; *Ribe and Christensen*, 1994]. The South Pacific super-swell also encompasses a number of hotspots: Marquesas, Society, Samoa, Austral, and Pitcairn (Figures 6c and 6d). Although not every hotspot is related to mantle plumes [*Courtillot et al.*, 2003] (but see *Davies* [2005]), it is evident that mantle plumes contribute significantly to these topographic swells.

[42] The question is whether the deviations from the HSC model are entirely caused by mantle convective upwelling plumes, as often suggested [*Schroeder*, 1984; *McNutt*, 1998]. To answer this question, we analyze the topography

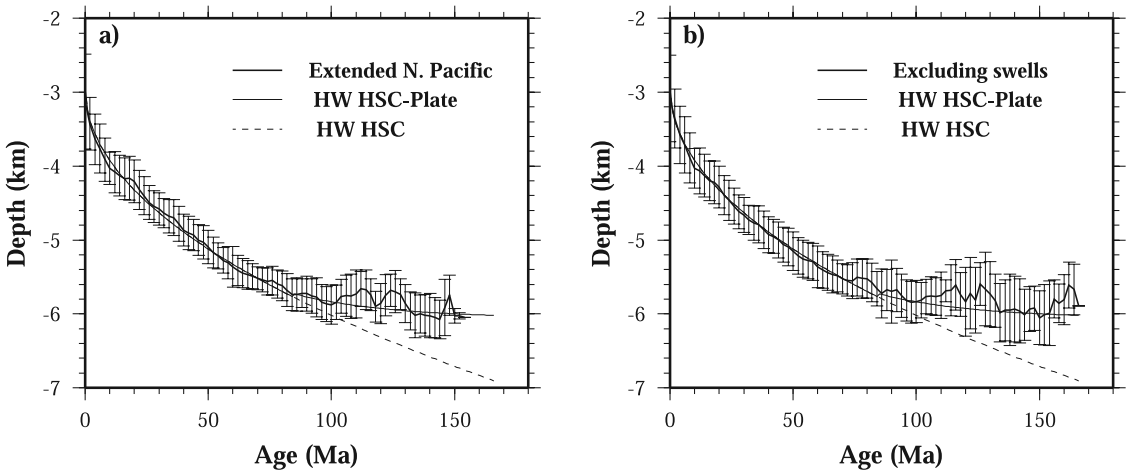

Figure 10. Mean depths and standard deviations in 2 Ma age bins versus seafloor age (a) for the expanded northern Pacific region (thick solid line) and (b) for the entire Pacific plate except the Hawaiian swell and South Pacific super-swell. The topography in Figures 10a and 10b is corrected for sediments, seamounts, and LIPs. Also plotted are HSC-Plate model (thin solid line) and HSC models (thin dashed line) by *Hillier and Watts* [2005]. In Figure 10b the Pacific curve is shifted down 0.1 km.

in the northern and southern regions of the Pacific plate (Figure 1c) where there are significantly fewer seamounts, LIPs and mantle plume activities. The depth-age relations show that significant deviations from the HSC predictions still exist for seafloor older than ~80 Ma in these two regions (Figures 4d, 4f, and 5a). One concern with this argument is the potential statistical bias that may be introduced by the much smaller area for old seafloor than for young seafloor in these two regions (Figure 2). This is in part caused by our intention to avoid the Darwin Rise, the South Pacific super-swell and the Hawaiian swell in dividing the northern and southern regions. Because the Darwin Rise after exclusion of seamounts and LIPs shows little positive residual topography with respect to the HW HSC-Plate model (Figure 7b), we may expand the northern region to include the adjacent portion of the Darwin Rise: west of 169° in longitude and north of 30°N, and repeat the analyses for the expanded northern region with a larger area for old seafloor. The resulting depth-age relation for the expanded northern region follows the same trend as the original depth-age relation and that in the HW HSC-Plate model (Figure 10a).

[43] We can take another approach to this question on the role of mantle plumes. Given that the Hawaiian swell and the South Pacific super-swell are most likely caused by mantle convective upwellings, we can exclude these two swells from our topography analyses (see Figure 6b for the approximate swell regions that are excluded). We do not exclude the Darwin Rise because it does not display significant topographic anomalies with respect to HW HSC-Plate model after removal of seamounts and LIPs (Figure 6b). The depth-age relation for the Pacific plate excluding these two swells again displays significant deviations from the HW HSC model, but follows HW HSC-Plate model well (Figure 10b and the curve for the Pacific is shifted down by 100 m). Compared to the depth-age relation for the entire Pacific plate (Figure 4c), the exclusion of the Hawaiian swell and South Pacific super-swell has the largest impact on topography between 70 Ma and 130 Ma where the exclusion of the swells reduces the topographic "flattening." This may reflect the fact that these two swells occupy the most area of seafloor younger than 130 Ma in our central region (Figure 6b). The exclusion of the Hawaiian swell and South Pacific super-swell effectively removes the large positive residual topography between 80 Ma and 130 Ma for residual topography with respect to the HW HSC-Plate model, and highlights the nearly monotonic increase with age after 70 Ma for residual topography with respect to the HSC models (Figures 7a and 7c).

[44] Another possible scenario is that the deviations at old seafloor are caused by residual heating of past plume materials that have spread out below the lithosphere and may still exist as a thin layer. This hypothesis is more difficult to test in the Pacific, because most of the seafloor older than 80 Ma is either on the downstream of the proposed Pacific plumes (e.g., the western Pacific and Darwin Rise) or in the vicinity of the two swells (e.g., the southern region) (Figure 6b). However, the seafloor between 80 Ma and 105 Ma northeast of the Hawaii-Emperor seamount chain in the northern region is unlikely affected by the Hawaiian swell but still shows significant positive residual topography with respect to the HSC model (Figures 6a and 5a) (note that the Hess Rise is excluded from the analyses). This suggests that the plume residual heating cannot be the main contributor to the deviations at old seafloor for this region.

[45] It has also been suggested, on the basis of extrapolation from the power law distribution of the plume population, that there were perhaps >5000 mantle plumes [*Malamud and Turcotte*, 1999] and that most of these plumes, although each individually is weak and small and is invisible to currently available geophysical detection methods, may collectively bring enough heat to the base of lithosphere to cause broad topographic anomalies to account for the topographic "flattening" [*Malamud and*

Turcotte, 1999]. However, this idea has been disputed recently and was considered as dynamically untenable on the basis of scaling analyses and modeling of the dynamics of mantle plumes that show that the plume population and plume spacing are fundamentally limited by mantle depth [*Zhong*, 2005].

[46] Finally, another line of evidence that is hard to reconcile with mantle plumes as the only cause for the deviations from the HSC model prediction is the nearly monotonic increase in residual topography with respect to HSC models with age starting from 70 Ma, and the large amplitudes of residual topography ($\sim$1.2 km at $\sim$160 Ma) (Figure 7c). This residual topography is significantly larger than the nearly uniform, age-independent standard deviations of corrected topography ($\sim$300 m) (Figure 7c), suggesting a different origin than the topographic variations at relatively young seafloor. If mantle plumes were the only cause for the deviations, then residual topography with respect to HSC models (e.g., Figures 6a and 7c) should all be caused by mantle plumes. Unless mantle plumes are preferentially located below old seafloor or plume materials accumulate below the lithosphere with time, it is difficult to explain this pattern of residual topography and its large amplitudes at old seafloor. However, there is no observational evidence for plumes to be preferentially located at old seafloor. In fact, most plumes are located near spreading centers, especially in the Atlantic [*Jellinek et al.*, 2003].

[47] Therefore we conclude that the deviations of seafloor topography from the HSC model prediction cannot be entirely caused by mantle convective upwellings, and other physical processes should play a role. The mean ocean depth after removal of seamounts, sediments, LIPs, and two clearly identified topography swells (Hawaiian and South Pacific) can be reasonably fit with the HSC-Plate model by *Hillier and Watts* [2005].

5.3. Plate Model and Its Physical Mechanisms

[48] We now assess other physical mechanisms that may cause the topography to deviate from the HSC model at old seafloor where no plume is present. Despite the impressive fit of Hillier and Watts' HSC-Plate model to the mean depths, the plate model does not address physical mechanisms that give rise to the required conditions for the plate model (i.e., constant temperature or constant heat flux at the base of lithosphere and a fixed plate thickness at old age). As reviewed in the introduction, until recently [*Huang and Zhong*, 2005], it was unclear whether the plate model is dynamically viable [*O'Connell and Hager*, 1980; *Davies*, 1988b, 1999].

[49] Sublithospheric small-scale convection (SSC) has been often suggested as the mechanism for the plate model [*Parsons and McKenzie*, 1978; *Yuen and Fleitout*, 1985; *Davaille and Jaupart*, 1994]. However, *O'Connell and Hager* [1980] and *Davies* [1988b, 1999] argued that although the SSC may limit the growth of lithospheric thickness by removing the bottom portion of the lithosphere, it may enhance the cooling of the underlying mantle, leading to either insignificant topographic deviations or even deepened topography compared to the HSC model prediction. This is because the topography is sensitive to integrated mantle buoyancy. The cooling effect of the SSC on the underlying mantle is observed both in numerical models [*Huang et al.*, 2003; *Huang and Zhong*, 2005] and in laboratory experiments [*Davaille and Jaupart*, 1994]. *Huang and Zhong* [2005] demonstrated that the SSC by itself indeed leads to no significant topographic deviations from the HSC model prediction, largely confirming the suggestion by *O'Connell and Hager* [1980].

[50] By formulating dynamic models for the mantle and lithosphere, *Huang and Zhong* [2005] examined the conditions that lead to mantle and lithospheric structures that are consistent with a plate model (i.e., constant lithospheric thickness and elevated topography and heat flux at old age and constant sublithospheric temperature). They found that for mantle convection with significant internal heating, additional heat, termed as "trapped" heat, tends to accumulate beneath old lithosphere. This "trapped" heat arises because the heat beneath old lithosphere, that is due partly to mantle volumetric (e.g., radiogenic) heating and partly to convective heat including that from mantle plumes, cannot be effectively released, hindered by thick lithosphere and lack in subduction cooling. This "trapped" heat generates elevated topography at old lithosphere relative to the HSC model prediction, irrespective of the presence of the SSC. However, when the asthenospheric viscosity is small enough ($\sim 10^{19}$ Pa s) to set on the SSC, the SSC may release the "trapped" heat by mixing the relatively cold, eroded bottom part of lithosphere with the underlying mantle containing the "trapped" heat. This process not only reheats the lithosphere, but also homogenizes the mantle temperature, leading to mantle and lithospheric conditions that are required by the plate model. This mechanism of lithospheric reheating associated with the "trapped" heat and SSC works well to reproduce the conditions for the plate model, provided that mantle convection has $>\sim$60% internal heating [*Huang and Zhong*, 2005]. Larger than $\sim$60% internal heating (i.e., the sum of radiogenic heating and heating from mantle secular cooling) for mantle convection is reasonable on the basis of the observations of plume heat flux and plume excess temperature [*Zhong*, 2006]. This suggests that the plate model is dynamically possible.

[51] It is worthwhile to emphasize that in the models by *Huang and Zhong* [2005] the "trapped" heat is responsible for producing the elevated topography relative to the HSC model even when the SSC is absent. The SSC's roles are to redistribute the heat in the mantle and lithosphere, homogenize mantle temperature, and erode/heat the base of the lithosphere. Therefore the SSC is the key to causing increased heat flux at old lithosphere [*Huang and Zhong*, 2005]. The "trapped" heat mechanism for producing topography anomalies is similar to that of incomplete homogenized thermal anomalies that was used by *Davies and Pribac* [1993] to explain the topographic variations of hundreds of meters along the MOR. However, the "trapped" heat was demonstrated to exist only below relatively old seafloor and is thus more relevant to explain the topographic deviations from the HSC model predictions at old seafloor [*Huang and Zhong*, 2005].

[52] Although seafloor topography at relatively old lithosphere requires that either lithosphere or the mantle or both be warmer below old seafloor than predicted from the HSC model, to distinguish the potential mechanisms (i.e., the plumes, "trapped" heat alone, "trapped" heat and SSC/

plate model, or other processes) that are responsible for the topographic anomalies demands other observations. Recently, *Priestley and McKenzie* [2006] demonstrated from a seismic surface wave study for the Pacific that the temperature at 150 km depth varies by no more than 20 K at ~1000 km length scale, supporting the plate model. *Ritzwoller et al.* [2004], using a thermal parameterization in surface wave tomographic inversion, found that the Pacific lithosphere older than 70 Ma on average is warmer than that from the HSC model prediction, suggesting lithospheric reheating. The age-dependence of averaged lithospheric structure from *Ritzwoller et al.* [2004] is consistent with the SSC with a power law rheology [*van Hunen et al.*, 2005]. Seafloor topography estimated from *Ritzwoller et al.* [2004] shows a general agreement with the observed topography, but differences also exist at mid-ocean ridges and other structurally complicated regions (Figure 9). Residual topography with respect to the seismically derived topography shows positive anomalies near the Hawaiian swell and South Pacific super-swell but with reduced area extent, compared to that with respect to the HW HSC-Plate model (Figure 6b). This may indicate that the seismically derived upper mantle and lithospheric structures recover some but not all of the plume materials in the shallow upper mantle. These results suggest that seafloor topography is controlled by shallow upper mantle and lithospheric structure and that the SSC plays an important role in thermal evolution of lithosphere.

[53] Heat flux, however, remains a key observation to distinguish among different physical mechanisms, despite the challenges to obtain accurate measurements owing to hydrological and hydrothermal effects [e.g., *Lister et al.*, 1990]. *Lister et al.* [1990] showed that heat flux for seafloor older than 110 Ma starts to deviate from the HSC prediction. While the SSC results in elevated heat flux at the surface after some delay from the onset of the SSC [*Davaille and Jaupart*, 1994; *Huang and Zhong*, 2005], it is unclear how efficiently plumes can erode lithosphere to increase surface heat flux. The Hawaiian swell does not show any significant heat flux anomalies [*von Herzen et al.*, 1989; *Harris et al.*, 2000], possibly because the plume heat has not yet been transferred through the lithosphere to the surface with heat conduction as the primary heat transfer mechanism [*Ribe and Christensen*, 1994]. However, more studies with realistic mantle rheology are needed to improve understanding of how the plumes and SSC may perturb the surface heat flux [*Moore et al.*, 1998].

6. Conclusions

[54] We analyzed the dependence of ocean depth on seafloor age for the Pacific plate. Using recently available data sets of high-resolution bathymetry, sediments, seamounts and large igneous provinces (LIP), we removed the effects of sediments, seamounts, and LIPs in our topography analyses. We divided the Pacific plate into northern, central, and southern regions to isolate the effects of seamounts and LIPs in the central region. We constructed maps of residual topography and analyzed residual topography. We also estimated the topography from seismic structure for the Pacific lithosphere and compared with the observed topography. The conclusions can be summarized as follows:

[55] 1. The age-averaged topography for the entire Pacific plate with sediments, seamounts, LIPs, the Hawaiian swell and South Pacific super-swell removed follows a cooling half-space model until 80–85 Ma, and the topography for older seafloor shows a reduced age dependence. In particular, the northern region that is not significantly affected by mantle plumes, seamounts, and LIPs (Figure 1c) also shows similar depth-age relation. The corrected topography shows nearly uniform standard deviations of ~300 m for all ages.

[56] 2. The mean-corrected ocean depths for the Pacific plate and also for the northern region can be fit reasonably well with a HSC-Plate depth-age relation recently developed for the North Pacific Ocean by *Hillier and Watts* [2005] with an entirely different approach than taken here (the North Pacific Ocean in the work of *Hillier and Watts* [2005] is for the entire Pacific Ocean north of the equator and is significantly larger than the northern region in our study).

[57] 3. Residual topography with Hillier and Watts' HSC-Plate model as a reference model shows two distinct topographic highs: the Hawaiian swell and the South Pacific super-swell, both of which are most likely caused by convective upwelling plumes. However, the Darwin Rise does not appear to be anomalously shallow, suggesting that the Darwin Rise is mainly due to densely populated seamounts and LIPs. The mean residual topography varies around zero for different ages and is comparable with ~300 m standard deviations in topography. However, while the residual topography with respect to the HSC models shows similarly small amplitudes for young seafloor, it displays 600–1500 m positive residual topography for old seafloor, much larger than ~300 m standard deviations in topography.

[58] 4. Estimated topography from the 3-D seismic model of the Pacific lithosphere and shallow upper mantle [*Ritzwoller et al.*, 2004] generally agrees with the observed topography, including the reduced topography at relatively old seafloor, suggesting that much of the topography away from the Hawaiian swell and the South Pacific super-swell is largely controlled by the thermal state of the lithosphere and the uppermost mantle.

[59] 5. While mantle plumes contribute to topographic deviations from the HSC model prediction, our results on the depth-age relation, residual topography, and the seismically derived topography suggest that the plumes cannot be the only cause for the topographic deviations. Our analyses, combined with seafloor heat flux data and seismic studies of the Pacific upper mantle structure, suggest that lithospheric reheating contributes significantly to the deviations. The "trapped" heat below old oceanic lithosphere may be responsible for reduced seafloor topography there. The "trapped" heat, coupled with SSC, may cause lithospheric reheating and lead to mantle and lithospheric conditions that are reasonably described by a plate model.

[60] Finally, we believe that to further improve our understanding on the cause of deviations of seafloor topography from the HSC model, more and better seismic observations on the oceanic upper mantle structure and reliable heat flux measurements at seafloor are necessary. More geodynamic modeling of plume-lithosphere interactions and SSC is also needed to better understand their effects on surface heat flux and topography.

[61] **Acknowledgments.** This research is supported by US-NSF grants EAR 0409217 and EAR 0134939 and the David and Lucile Packard Foundation. The authors would like to thank M. Coffin for providing the LIP data set, G. Nolet and J. Ritsema for their seismic models, and Geoff Davies and J. Hillier for critical and constructive reviews that helped to improve the paper significantly.

References

Caress, D. W., M. K. McNutt, R. S. Detrick, and J. C. Mutter (1995), Seismic imaging of hotspot-related crustal underplating beneath the Marquesas Islands, *Nature*, *373*, 600–603.

Carlson, R. L., and H. P. Johnson (1994), On modeling the thermal evolution of the oceanic upper mantle: An assessment of the cooling plate model, *J. Geophys. Res.*, *99*, 3201–3214.

Coffin, M. F., and O. Eldholm (1994), Large igneous provinces: Crustal structure, dimensions, and external consequences, *Rev. Geophys.*, *32*, 1–36.

Courtillot, V., A. Davaille, J. Besse, and J. Stock (2003), Three distinct types of hotspots in the Earth's mantle, *Earth Planet. Sci. Lett.*, *205*, 295–308.

Crosby, A. G., D. McKenzie, and J. G. Sclater (2006), The relationship between depth, age and gravity in the oceans, *Geophys. J. Int.*, *166*, 553–573.

Davaille, A., and C. Jaupart (1994), Onset of thermal convection in fluids with temperature-dependent viscosity: Application to the oceanic mantle, *J. Geophys. Res.*, *99*, 19,853–19,866.

Davies, G. F. (1988a), Ocean bathymetry and mantle convection: 1. Large-scale flow and hotspots, *J. Geophys. Res.*, *93*, 10,467–10,480.

Davies, G. F. (1988b), Ocean bathymetry and mantle convection: 2. Small-scale flow, *J. Geophys. Res.*, *93*, 10,481–10,488.

Davies, G. F. (1999), *Dynamic Earth: Plates, Plumes and Mantle Convection*, Cambridge Univ. Press, New York.

Davies, G. F. (2005), A case for mantle plumes, *Chin. Sci. Bull.*, *50*, 1541–1554.

Davies, G. F., and F. Pribac (1993), Mesozoic seafloor subsidence and the Darwin Rise, past and present, in *The Mesozoic Pacific*, *Geophys. Monogr. Ser.*, vol. 77, edited by M. Pringle et al., pp. 39–52, AGU, Washington, D. C.

Doin, M. P., and L. Fleitout (2000), Flattening of the oceanic topography and geoid: Thermal versus dynamic origin, *Geophys. J. Int.*, *143*, 582–594.

Dumoulin, C., M. P. Doin, and L. Fleitout (2001), Numerical simulations of the cooling of an oceanic lithosphere above a convective mantle, *Phys. Earth Planet. Int.*, *125*, 45–64.

Harris, R. N., R. P. Von Herzen, M. K. McNutt, G. Garven, and K. Jordahl (2000), Submarine hydrogeology of the Hawaiian archipelagic apron: 1. Heat flow patterns north of Oahu and Maro Reef, *J. Geophys. Res.*, *105*, 21,353–21,369.

Heestand, R. L., and T. S. Crough (1981), The effect of hot spots on the oceanic age-depth relation, *J. Geophys. Res.*, *86*, 76,107–76,114.

Hillier, J. K., and A. B. Watts (2004), "Plate-like" subsidence of the East Pacific Rise–South Pacific Superswell system, *J. Geophys. Res.*, *109*, B10102, doi:10.1029/2004JB003041.

Hillier, J. K., and A. B. Watts (2005), Relationship between depth and age in the North Pacific Ocean, *J. Geophys. Res.*, *110*, B02405, doi:10.1029/2004JB003406.

Huang, J., and S. Zhong (2005), Sublithospheric small-scale convection and its implications for residual topography at old ocean basins and the plate model, *J. Geophys. Res.*, *110*, B05404, doi:10.1029/2004JB003153.

Huang, J., S. Zhong, and J. van Hunen (2003), Controls on sublithospheric small-scale convection, *J. Geophys. Res.*, *108*(B8), 2405, doi:10.1029/2003JB002456.

Jellinek, A. M., H. M. Gonnermann, and M. A. Richards (2003), Plume capture by divergent plate motions: Implications for the distribution of hotspots, geochemistry of mid-ocean ridge basalts, and estimates of the heat flux at the core-mantle boundary, *Earth Planet. Sci. Lett.*, *205*, 361–378.

Leahy, M. L., and J. Park (2005), Hunting for oceanic island Moho, *Geophys. J. Int.*, *160*, 1020–1026.

Lister, C. R. B., J. G. Sclater, E. E. Davis, H. Villinger, and S. Nagihara (1990), Heat flow maintained in ocean basins of great age: Investigations in the north-equatorial west Pacific, *Geophys. J. Int.*, *102*, 603–630.

Lithgow-Bertelloni, C., and P. G. Silver (1998), Dynamic topography, plate driving forces and the African superswell, *Nature*, *395*, 269–272.

Malamud, B. D., and D. L. Turcotte (1999), How many plumes are there?, *Earth Planet. Sci. Lett.*, *174*, 113–124.

Marty, J. C., and A. Cazenave (1989), Regional variations in subsidence rate of oceanic plates: A global analysis, *Earth Planet. Sci. Lett.*, *94*, 301–315.

McKenzie, D. P. (1967), Some remarks on heat flow and gravity anomalies, *J. Geophys. Res.*, *72*, 6261–6273.

McNutt, M. K. (1998), Superswell, *Rev. Geophys*, *36*, 211–244.

Menard, H. W. (1964), *Marine Geology of the Pacific*, 271 pp., McGraw-Hill, New York.

Montelli, R., G. Nolet, F. A. Dahlen, G. Masters, E. R. Engdahl, and S. H. Hung (2004), Finite frequency tomography reveals a variety of plumes in the mantle, *Science*, *303*, 338–343.

Montelli, R., G. Nolet, F. A. Dahlen, and G. Masters (2006), A catalogue of deep mantle plumes: New results from finite-frequency tomography, *Geochem. Geophys. Geosyst.*, *7*, Q11007, doi:10.1029/2006GC001248.

Moore, W. B., G. Schubert, and P. Tackley (1998), Three-dimensional simulations of plume-lithosphere interaction at Hawaiian Swell, *Science*, *279*, 1008–1011.

Morgan, W. J. (1972), Plate motions and deep mantle convection, *Mem. Geol. Soc. Am.*, *132*, 7–22.

Müller, R. D., W. R. Roest, J.-Y. Royer, L. M. Gahagan, and J. G. Sclater (1997), Digital isochrons of the world's ocean floor, *J. Geophys. Res.*, *102*, 3211–3214.

National Geophysics Data Center (NGDC) (2003), Total sediment thickness of the world's oceans and marginal seas, http://www.ngdc.noaa.gov/mgg/sedthick/sedthick.html, Boulder, Colo.

O'Connell, R. J., and B. H. Hager (1980), On the thermal state of the Earth, in *Physics of the Earth's Interior*, edited by A. Dziewonski and E. Boschi, pp. 270–317, Elsevier, New York.

Olson, P. (1990), Hot spots, swells and mantle plumes, in *Magma Transport and Storage*, edited by M. P. Ryan, pp. 33–51, John Wiley, Hoboken, N. J.

Panasyuk, S. V., and B. Hager (2000), Models of isostatic and dynamic topography, geoid anomalies, and their uncertainties, *J. Geophys. Res.*, *105*, 28,199–28,209.

Parsons, B., and D. McKenzie (1978), Mantle convection and thermal structure of the plates, *J. Geophys. Res.*, *83*, 4485–4496.

Parsons, B., and J. G. Sclater (1977), An analysis of the variation of ocean floor bathymetry and heat flow with age, *J. Geophys. Res.*, *82*, 803–827.

Priestley, K., and D. McKenzie (2006), The thermal structure of the lithosphere from shear wave velocities, *Earth Planet. Sci. Lett.*, *244*, 285–301.

Renkin, M. L., and J. G. Sclater (1988), Depth and age in the North Pacific, *J. Geophys. Res.*, *93*, 2910–2935.

Ribe, N. M., and U. R. Christensen (1994), Three-dimensional modeling of plume-lithosphere interaction, *J. Geophys. Res.*, *99*, 669–683.

Ritsema, J., H. J. van Heijst, and J. H. Woodhouse (1999), Complex shear wave velocity structure imaged beneath Africa and Iceland, *Science*, *286*, 1925–1928.

Ritzwoller, M. H., N. M. Shapiro, and S. Zhong (2004), Cooling history of the Pacific lithosphere, *Earth Planet. Sci. Lett.*, *226*, 69–84.

Romanowicz, B., and Y. C. Gung (2002), Superplumes from the core-mantle boundary to the lithosphere: Implications for heat flux, *Science*, *296*, 513–516.

Schroeder, W. (1984), The empirical age-depth relation and depth anomalies in the Pacific Ocean basin, *J. Geophys. Res.*, *89*, 9873–9883.

Shapiro, N. M., and M. H. Ritzwoller (2004), Thermodynamic constraints on seismic inversions, *Geophys. J. Int.*, *157*, 1175–1188.

Sleep, N. H. (1990), Hotspots and mantle plumes: Some phenomenology, *J. Geophys. Res.*, *95*, 6715–6736.

Smith, W. H. F., and D. T. Sandwell (1997), Global sea floor topography from satellite altimetry and ship depth soundings, *Science*, *277*, 1956–1962.

Stein, C. A., and S. Stein (1992), A model for the global variation in oceanic depth and heat flow with lithospheric age, *Nature*, *359*, 123–129.

ten Brink, U. S., and T. M. Brocher (1987), Multichannel seismic evidence for a subcrustal intrusive complex under Oahu and a model for Hawaiian volcanism, *J. Geophys. Res.*, *92*, 13,687–13,707.

van Hunen, J., S. Zhong, N. M. Shapiro, and M. H. Ritzwoller (2005), New evidence for dislocation creep from 3-D geodynamic modeling the Pacific upper mantle structure, *Earth Planet. Sci., Lett.*, *238*, 146–155.

von Herzen, R. P., M. J. Cordery, R. S. Detrick, and C. Fang (1989), Heat flow and the thermal origin of hot spot swells: The Hawaiian swell revisited, *J. Geophys. Res.*, *94*, 13,783–13,799.

Wessel, P. (2001), Global distribution of seamounts inferred from gridded Geosat/ERS-1 altimetry, *J. Geophys. Res.*, *106*, 19,431–19,441.

Wolfe, C. J., I. T. Bjarnason, J. C. Vandecar, and S. C. Soloman (1997), Seismic structure of the Iceland mantle plume, *Nature*, *385*, 245–247.

Yuen, D. A., and L. Fleitout (1985), Thinning of the lithosphere by small-scale convective destabilization, *Nature*, *313*, 125–128.

Zhong, S. (2005), Dynamics of thermal plumes in 3D isoviscous thermal convection, *Geophys. J. Int.*, *162*, 289–300.

Zhong, S. (2006), Constraints on thermochemical convection of the mantle from plume heat flux, plume excess temperature and upper mantle temperature, *J. Geophys. Res.*, *111*, B04409, doi:10.1029/2005JB003972.

Zhong, S., and A. B. Watts (2002), Constraints on the dynamics of mantle plumes from uplift of Hawaiian islands, *Earth Planet. Sci. Lett.*, *203*, 105–116.

J. Huang, Research School of Earth Sciences, Australian National University, Canberra, ACT 0200, Australia.

W. Landuyt, Department of Geology and Geophysics, Yale University, New Haven, CT 06520, USA.

M. Ritzwoller and S. Zhong, Department of Physics, University of Colorado, Boulder, CO 80309, USA. (szhong@colorado.edu)

N. Shapiro, Institut de Physique du Globe, 4 Place Jussieu, 75252 Paris cedex 05, France.

P. Wessel, Department of Geology and Geophysics, SOEST, University of Hawaii at Manoa, Honolulu, HI 96822, USA.